

# Dissipativity-Based Distributed Control and Communication Topology Co-Design for Voltage Regulation and Current Sharing in DC Microgrids

Mohammad Javad Najafirad and Shirantha Welikala

**Abstract**—This paper presents a novel dissipativity-based distributed droop-free control approach for voltage regulation and current sharing in DC microgrids (MGs) comprised of an interconnected set of distributed generators (DGs), loads, and power lines. First, we describe the closed-loop DC MG as a networked system where the DGs and lines (i.e., subsystems) are interconnected via a static interconnection matrix. This interconnection matrix demonstrates how the inputs, outputs, and disturbances of DGs and lines are connected in a DC MG. Each DG has a local controller and a distributed global controller. To design the controller, we use the dissipativity properties of the subsystems and formulate a linear matrix inequality (LMI) problem. To support the feasibility of this problem, we identify a set of necessary local and global conditions that we then enforce in a specifically developed LMI-based controller design process. In contrast to existing DC MG control solutions, our approach proposes a unified framework for co-designing the distributed controller and communication topology. As the co-design process is LMI-based, it can be efficiently implemented and evaluated. The effectiveness of the proposed solution can be verified by simulating an islanded DC MG in a MATLAB/Simulink environment under different scenarios, such as load changes and topological constraint changes, and then comparing the performance with a recent droop control algorithm.

**Index Terms**—DC Microgrid, Power Systems, Voltage Regulation, Distributed Control, Networked Systems, Dissipativity-Based Control, Topology Design.

## I. INTRODUCTION

Microgrids (MG) integrate distributed generators (DG) that include photovoltaics, wind turbines, fuel cells, and microturbines, with energy storage systems and local loads into a controllable network [1]. DC MGs offer superior advantages over AC systems by eliminating unnecessary conversion stages, avoiding frequency regulation and synchronization challenges, and enabling more straightforward control strategies due to resistive line characteristics. This architecture improves reliability, efficiency, and scalability while supporting existing AC infrastructure, making DC microgrids increasingly favorable for modern integration of renewable energy.

DC MGs face two main control challenges: voltage regulation and current sharing among distributed generators (DGs). To address these, researchers have developed centralized [2], decentralized [3], and distributed control [4] strategies. Although centralized control provides precise performance, it

lacks resilience against single-point failures and limits plug-and-play functionality [5]. Decentralized approaches eliminate the need for global information, but often compromise the accuracy of current sharing [6]. Droop control, a widely adopted decentralized strategy, enables proportional current sharing without requiring direct communication [5]. Distributed control overcomes these limitations by allowing DGs to exchange information through a sparse communication network, enhancing reliability, flexibility, and scalability in DC MGs [7].

A significant limitation of droop control in DC MGs is the inherent compromise between voltage regulation and current sharing performance. This challenge becomes particularly pronounced in low-voltage DC systems, where the variation of line impedances further complicates the control dynamics [8]. Although researchers have developed modified droop control strategies that incorporate communication networks to address these limitations [9], such approaches often introduce additional system complexity and implementation costs. Secondary control integration has been proposed to enhance voltage regulation and current sharing accuracy [10], but this solution increases communication requirements and system overhead. Event-triggered algorithms represent a promising direction for reducing communication burden among DGs [11]. Despite these innovations, droop control fundamentally requires careful tuning of droop coefficients to effectively balance the conflicting objectives of voltage regulation while ensuring proper current sharing among DGs.

Furthermore, conventional distributed controller design typically proceeds independently from communication topology considerations, with network structures often assumed to be static or predetermined. This approach, however, fails to account for the practical reality that communication topologies may fluctuate due to the inherently intermittent nature of DGs. Recent advancements in communication technologies, particularly software-defined radio networks, have eliminated the necessity for fixed communication structures. This newfound flexibility creates opportunities for developing innovative control strategies that can advantageously utilize customizable and reconfigurable communication topologies, potentially leading to more robust and efficient MG operation across varying operational conditions.

This paper introduces a novel dissipativity-based distributed droop-free control framework that addresses the aforementioned limitations by eliminating the need for droop characteristics. Instead of conventional approaches, the pro-

The authors are with the Department of Electrical and Computer Engineering, School of Engineering and Science, Stevens Institute of Technology, Hoboken, NJ 07030, {mnajafir, swelikala}@stevens.edu.

posed methodology conceptualizes DGs, loads, and transmission lines as interconnected energy systems, focusing on their fundamental energy interactions. Applying dissipativity principles from system theory provides a comprehensive model that ensures system stability and optimal power flow throughout the DC MG. This energy-centric approach offers a more elegant solution to voltage regulation and current sharing challenges without the traditional compromises inherent in droop-based control strategies.

This paper proposes an innovative co-design methodology that simultaneously optimizes distributed controllers and communication topology in DC microgrids. By formulating this dual-aspect challenge as a linear matrix inequality (LMI) problem, we ensure robust system performance with an optimized communication network. The resulting framework enables efficient, decentralized, and compositional implementation across MGs.

The main contributions of this paper can be outlined as:

- 1) We formulate the DC MG control problem as a hierarchical networked system control problem and propose a novel framework that combines local voltage control with distributed consensus-based current sharing through a co-design approach.
- 2) We develop a comprehensive hierarchical control strategy including local voltage controllers, distributed consensus-based controllers, and a systematic LMI-based design technique for controller synthesis that ensures both voltage regulation and proportional current sharing.
- 3) We present a dissipativity-based approach that eliminates the need for traditional droop control, improving voltage regulation accuracy and current sharing while enhancing overall system stability through optimized communication topology.
- 4) We formulate all design problems as LMI-based convex optimization problems, enabling efficient numerical implementation, scalable controller synthesis, systematic stability analysis, and joint optimization of control gains and communication topology [12].

Besides, the proposed DC MG control framework is grounded on generic dissipativity, networked systems, and LMI techniques. Thus it has a high potential for future development, e.g., to effectively handle complex components (via dissipativity [13] and PnP (via decentralization [14])).

This paper is structured as follows. Section II covers necessary preliminary concepts on dissipativity and networked systems. Section III presents the DC MG modeling and co-design problem formulation. The hierarchical control design and stability analysis are presented in Section V. The dissipativity-based distributed control and topology co-design approach is detailed in Section VI. Simulation results are presented in Section VII, followed by conclusions in Section VIII.

## II. PRELIMINARIES

**Notations:** The notation  $\mathbb{R}$  and  $\mathbb{N}$  signify the sets of real and natural numbers, respectively. For any  $N \in \mathbb{N}$ , we define

$\mathbb{N}_N \triangleq \{1, 2, \dots, N\}$ . An  $n \times m$  block matrix  $A$  is denoted as  $A = [A_{ij}]_{i \in \mathbb{N}_n, j \in \mathbb{N}_m}$ . Either subscripts or superscripts are used for indexing purposes, e.g.,  $A_{ij} = A^{ij}$ .  $[A_{ij}]_{j \in \mathbb{N}_m}$  and  $\text{diag}([A_{ii}]_{i \in \mathbb{N}_n})$  represent a block row matrix and a block diagonal matrix, respectively.  $\mathbf{0}$  and  $\mathbf{I}$ , respectively, are the zero and identity matrices (dimensions will be clear from the context). A symmetric positive definite (semi-definite) matrix  $A \in \mathbb{R}^{n \times n}$  is denoted by  $A > 0$  ( $A \geq 0$ ). The symbol  $\star$  represents conjugate blocks inside block a symmetric matrices,  $\mathcal{H}(A) \triangleq A + A^\top$  and  $\mathbf{1}_{\{\cdot\}}$  is the indicator function.

### A. Dissipativity

Consider a general non-linear dynamic system

$$\begin{aligned} \dot{x}(t) &= f(x(t), u(t)), \\ y(t) &= h(x(t), u(t)), \end{aligned} \quad (1)$$

where  $x(t) \in \mathbb{R}^n$ ,  $u(t) \in \mathbb{R}^q$ ,  $y(t) \in \mathbb{R}^m$ , and  $f: \mathbb{R}^n \times \mathbb{R}^q \rightarrow \mathbb{R}^n$  and  $h: \mathbb{R}^n \times \mathbb{R}^q \rightarrow \mathbb{R}^m$  are continuously differentiable.

The equilibrium points of (1) are such that there is a unique  $u^* \in \mathbb{R}^q$  such that  $f(x^*, u^*) = 0$  for any  $x^* \in \mathcal{X}$ , where  $\mathcal{X} \subset \mathbb{R}^n$  is the set of equilibrium states. And both  $u^*$  and  $y^* \triangleq h(x^*, u^*)$  are implicit functions of  $x^*$ .

The *equilibrium-independent-dissipativity* (EID) [15] is defined next to examine dissipativity of (1) without the explicit knowledge of its equilibrium points.

**Definition 1:** The system (1) is called EID under supply rate  $s: \mathbb{R}^q \times \mathbb{R}^m \rightarrow \mathbb{R}$  if there is a continuously differentiable storage function  $V: \mathbb{R}^n \times \mathcal{X} \rightarrow \mathbb{R}$  such that  $V(x, x^*) > 0$  when  $x \neq x^*$ ,  $V(x^*, x^*) = 0$ , and

$$\dot{V}(x, x^*) = \nabla_x V(x, x^*) f(x, u) \leq s(u - u^*, y - y^*),$$

for all  $(x, x^*, u) \in \mathbb{R}^n \times \mathcal{X} \times \mathbb{R}^q$ .

This EID property can be specialized based on the used supply rate  $s(\cdot, \cdot)$ . The *X-EID* property, defined in the sequel, uses a quadratic supply rate determined by a coefficient matrix  $X = X^\top \triangleq [X^{kl}]_{k, l \in \mathbb{N}_2} \in \mathbb{R}^{q+m}$  [13].

**Definition 2:** The system (1) is *X-EID* if it is EID under the quadratic supply rate:

$$s(u - u^*, y - y^*) \triangleq \begin{bmatrix} u - u^* \\ y - y^* \end{bmatrix}^\top \begin{bmatrix} X^{11} & X^{12} \\ X^{21} & X^{22} \end{bmatrix} \begin{bmatrix} u - u^* \\ y - y^* \end{bmatrix}.$$

**Remark 1:** If the system (1) is *X-EID* with:

- 1)  $X = \begin{bmatrix} \mathbf{0} & \frac{1}{2}\mathbf{I} \\ \frac{1}{2}\mathbf{I} & \mathbf{0} \end{bmatrix}$ , then it is passive;
- 2)  $X = \begin{bmatrix} -\nu\mathbf{I} & \frac{1}{2}\mathbf{I} \\ \frac{1}{2}\mathbf{I} & -\rho\mathbf{I} \end{bmatrix}$ , then it is strictly passive ( $\nu$  and  $\rho$  are the input and output passivity indices, denoted as IF-OPF( $\nu, \rho$ ));
- 3)  $X = \begin{bmatrix} \gamma^2\mathbf{I} & \mathbf{0} \\ \mathbf{0} & -\mathbf{I} \end{bmatrix}$ , then it is  $L_2$ -stable ( $\gamma$  is the  $L_2$ -gain, denoted as  $L_2G(\gamma)$ );

in an equilibrium-independent manner (see also [16]).

If the system (1) is linear time-invariant (LTI), a necessary and sufficient condition for *X-EID* is provided in the following proposition as a linear matrix inequality (LMI) problem.

**Proposition 1:** [17] The LTI system

$$\dot{x}(t) = Ax(t) + Bu(t), \quad y(t) = Cx(t) + Du(t),$$

is *X-EID* if and only if there exists  $P > 0$  such that

$$\begin{bmatrix} -\mathcal{H}(PA) + C^\top X^{22} C & -PB + C^\top X^{21} + C^\top X^{22} D \\ \star & X^{11} + \mathcal{H}(X^{12} D) + D^\top X^{22} D \end{bmatrix} \geq 0.$$

The following corollary considers a specific LTI system with a local controller (a setup useful later) and formulates an LMI problem for *X-EID* enforcing local controller synthesis.

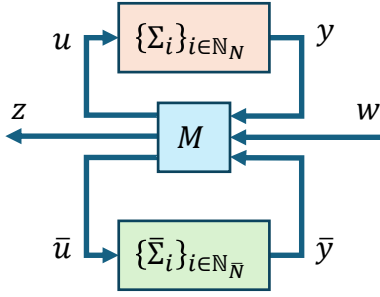


Fig. 1. A generic networked system  $\Sigma$ .

**Corollary 1:** [17] The LTI system

$$\dot{x}(t) = (A + BL)x(t) + \eta(t), \quad y(t) = x(t),$$

is  $X$ -EID with  $X^{22} < 0$  if and only if there exists  $P > 0$  and  $K$  such that

$$\begin{bmatrix} -(X^{22})^{-1} & P & 0 \\ * & -\mathcal{H}(AP + BK) & -\mathbf{I} + PX^{21} \\ * & * & X^{11} \end{bmatrix} \geq 0,$$

and  $L = KP^{-1}$ .

### B. Networked Systems

Consider the networked system  $\Sigma$  in Fig. 1, consisting of dynamic subsystems  $\Sigma_i, i \in \mathbb{N}_N$ ,  $\bar{\Sigma}_i, i \in \mathbb{N}_{\bar{N}}$  and a static interconnection matrix  $M$  that characterizes interconnections among subsystems, exogenous inputs  $w(t) \in \mathbb{R}^r$  (e.g. disturbances) and interested outputs  $z(t) \in \mathbb{R}^l$  (e.g. performance).

The dynamics of each subsystem  $\Sigma_i, i \in \mathbb{N}_N$  are given by

$$\begin{aligned} \dot{x}_i(t) &= f_i(x_i(t), u_i(t)), \\ y_i(t) &= h_i(x_i(t), u_i(t)), \end{aligned} \quad (2)$$

where  $x_i(t) \in \mathbb{R}^{n_i}$ ,  $u_i(t) \in \mathbb{R}^{q_i}$ ,  $y_i(t) \in \mathbb{R}^{m_i}$ . Similar to (1), each subsystem  $\Sigma_i, i \in \mathbb{N}_N$  is considered to have a set  $\mathcal{X}_i \subset \mathbb{R}^{n_i}$ , where for every  $x_i^* \in \mathcal{X}_i$ , there exists a unique  $u_i^* \in \mathbb{R}^{q_i}$  such that  $f_i(x_i^*, u_i^*) = 0$ , and both  $u_i^*$  and  $y_i^* \triangleq h_i(x_i^*, u_i^*)$  are implicit function of  $x_i^*$ . Moreover, each subsystem  $\Sigma_i, i \in \mathbb{N}_N$  is assumed to be  $X_i$ -EID, where  $X_i \triangleq [X_i^{kl}]_{k,l \in \mathbb{N}_2}$ . Regarding each subsystem  $\bar{\Sigma}_i, i \in \mathbb{N}_{\bar{N}}$ , we use similar assumptions and notations, but include a bar symbol to distinguish between the two types of subsystems, e.g.,  $\bar{\Sigma}_i$  is assumed to be  $\bar{X}_i$ -EID where  $\bar{X}_i \triangleq [\bar{X}_i^{kl}]_{k,l \in \mathbb{N}_2}$ .

Defining  $u \triangleq [u_i^\top]_{i \in \mathbb{N}_N}^\top$ ,  $y \triangleq [y_i^\top]_{i \in \mathbb{N}_N}^\top$ ,  $\bar{u} \triangleq [\bar{u}_i^\top]_{i \in \mathbb{N}_{\bar{N}}}^\top$  and  $\bar{y} \triangleq [\bar{y}_i^\top]_{i \in \mathbb{N}_{\bar{N}}}^\top$ , the interconnection matrix  $M$  and the corresponding interconnection relationship are given by

$$\begin{bmatrix} u \\ \bar{u} \\ z \end{bmatrix} = M \begin{bmatrix} y \\ \bar{y} \\ w \end{bmatrix} \equiv \begin{bmatrix} M_{uy} & M_{u\bar{y}} & M_{uw} \\ M_{\bar{u}y} & M_{\bar{u}\bar{y}} & M_{\bar{u}w} \\ M_{zy} & M_{z\bar{y}} & M_{zw} \end{bmatrix} \begin{bmatrix} y \\ \bar{y} \\ w \end{bmatrix}. \quad (3)$$

The following proposition exploits the  $X_i$ -EID and  $\bar{X}_i$ -EID properties of the subsystems  $\Sigma_i, i \in \mathbb{N}_N$  and  $\bar{\Sigma}_i, i \in \mathbb{N}_{\bar{N}}$  to formulate an LMI problem for synthesizing the interconnection matrix  $M$  (3), ensuring the networked system  $\Sigma$  is  $\mathbf{Y}$ -EID for a prespecified  $\mathbf{Y}$  under two mild assumptions [13].

**Assumption 1:** For the networked system  $\Sigma$ , the provided  $\mathbf{Y}$ -EID specification is such that  $\mathbf{Y}^{22} < 0$ .

**Remark 2:** Based on Rm. 1, As. 1 holds if the networked system  $\Sigma$  must be either: (i) L2G( $\gamma$ ) or (ii) IF-OFP( $\nu, \rho$ ) with some  $\rho > 0$ , i.e.,  $L_2$ -stable or passive, respectively. Therefore, As. 1 is mild since it is usually preferable to make the networked system  $\Sigma$  either  $L_2$ -stable or passive.

**Assumption 2:** In the networked system  $\Sigma$ , each subsystem  $\Sigma_i$  is  $X_i$ -EID with  $X_i^{11} > 0, \forall i \in \mathbb{N}_N$ , and similarly, each subsystem  $\bar{\Sigma}_i$  is  $\bar{X}_i$ -EID with  $\bar{X}_i^{11} > 0, \forall i \in \mathbb{N}_{\bar{N}}$ .

**Remark 3:** According to Rm. 1, As. 2 holds if a subsystem  $\Sigma_i, i \in \mathbb{N}_N$  is either: (i) L2G( $\gamma_i$ ) or (ii) IF-OFP( $\nu_i, \rho_i$ ) with  $\nu_i < 0$  (i.e.,  $L_2$ -stable or non-passive). Since in passivity-based control, often the involved subsystems are non-passive (or can be treated as such), As. 2 is also mild.

**Proposition 2:** [13] Under As. 1, the error network system  $\bar{\Sigma}$  can be made stable by synthesizing the interconnection matrix  $M$  via solving the LMI problem:

$$\text{Find: } L_{uy}, L_{u\bar{y}}, L_{\bar{u}y}, L_{\bar{u}\bar{y}}, \quad (4)$$

$$\text{Sub. to: } p_i \geq 0, \forall i \in \mathbb{N}_N, \quad \bar{p}_l \geq 0, \forall l \in \mathbb{N}_{\bar{N}}, \text{ and (5),}$$

$$\text{with } \begin{bmatrix} M_{uy} & M_{u\bar{y}} \\ M_{\bar{u}y} & M_{\bar{u}\bar{y}} \end{bmatrix} = \begin{bmatrix} \bar{\mathbf{X}}_p^{11} & \mathbf{0} \\ \mathbf{0} & \bar{\mathbf{X}}_{\bar{p}}^{11} \end{bmatrix}^{-1} \begin{bmatrix} L_{uy} & L_{u\bar{y}} \\ L_{\bar{u}y} & L_{\bar{u}\bar{y}} \end{bmatrix}.$$

**Proposition 3:** [13] Under As. 1-2, the network system  $\Sigma$  can be made  $\mathbf{Y}$ -EID (from  $w(t)$  to  $z(t)$ ) by synthesizing the interconnection matrix  $M$  (3) via solving the LMI problem:

$$\text{Find: } L_{uy}, L_{u\bar{y}}, L_{uw}, L_{\bar{u}y}, L_{\bar{u}\bar{y}}, L_{\bar{u}w}, M_{zy}, M_{z\bar{y}}, M_{zw}, \quad (6)$$

$$\text{Sub. to: } p_i \geq 0, \forall i \in \mathbb{N}_N, \quad \bar{p}_l \geq 0, \forall l \in \mathbb{N}_{\bar{N}}, \text{ and (7),}$$

$$\text{with } \begin{bmatrix} M_{uy} & M_{u\bar{y}} & M_{uw} \\ M_{\bar{u}y} & M_{\bar{u}\bar{y}} & M_{\bar{u}w} \end{bmatrix} = \begin{bmatrix} \mathbf{X}_p^{11} & \mathbf{0} \\ \mathbf{0} & \bar{\mathbf{X}}_{\bar{p}}^{11} \end{bmatrix}^{-1} \begin{bmatrix} L_{uy} & L_{u\bar{y}} & L_{uw} \\ L_{\bar{u}y} & L_{\bar{u}\bar{y}} & L_{\bar{u}w} \end{bmatrix}.$$

## III. PROBLEM FORMULATION

This section presents the dynamic modeling of the DC MG, which consists of multiple DGs, loads, and transmission lines. Specifically, our modeling approach is motivated by [18], which highlights the role and impact of communication and physical topologies in DC MGs. We also introduce local and global controllers for the DC MG and represent the closed-loop DC MG as a networked system.

### A. DC MG Physical Interconnection Topology

The physical interconnection topology of a DC MG is modeled as a directed connected graph  $\mathcal{G}^p = (\mathcal{V}, \mathcal{E})$  where  $\mathcal{V} = \mathcal{D} \cup \mathcal{L}$  is bipartite:  $\mathcal{D} = \{\Sigma_i^{DG}, i \in \mathbb{N}_N\}$  (DGs) and  $\mathcal{L} = \{\Sigma_l^{line}, l \in \mathbb{N}_L\}$  (transmission lines). The DGs are interconnected with each other through transmission lines. The interface between each DG and the DC MG is through a point of common coupling (PCC). For simplicity, the loads are assumed to be connected to the DG terminals at the respective PCCs [19]. Indeed loads can be moved to PCCs using Kron reduction even if they are located elsewhere [19].

To represent the DC MG's physical topology, we use its adjacency matrix  $\mathcal{A} = \begin{bmatrix} \mathbf{0} & \mathcal{B} \\ \mathcal{B}^\top & \mathbf{0} \end{bmatrix}$ , where  $\mathcal{B} \in \mathbb{R}^{N \times L}$  is the incident matrix of the DG network (where nodes are just the DGs and edges are just the transmission lines). Note that  $\mathcal{B}$  is also known as the "bi-adjacency" matrix of  $\mathcal{G}^p$  that describes the connectivity between its two types of nodes. In particular,  $\mathcal{B} = [\mathcal{B}_{il}]_{i \in \mathbb{N}_N, l \in \mathbb{N}_L}$  with  $\mathcal{B}_{il} \triangleq \mathbf{1}_{\{l \in \mathcal{E}_i^+\}} - \mathbf{1}_{\{l \in \mathcal{E}_i^-\}}$ , where  $\mathcal{E}_i^+$  and  $\mathcal{E}_i^-$  represent the out- and in-neighbors of  $\Sigma_i^{DG}$ .

### B. Dynamic Model of a Distributed Generator (DG)

Each DG consists of a DC voltage source, a voltage source converter (VSC), and some RLC components. Each DG  $\Sigma_i^{DG}, i \in \mathbb{N}_N$  supplies power to a specific load at its PCC

(denoted  $PCC_i$ ). Additionally, it interconnects with other DG units via transmission lines  $\{\Sigma_l^{line} : l \in \mathcal{E}_i\}$ . Figure 2 illustrates the schematic diagram of  $\Sigma_i^{DG}$ , including the local load, a connected transmission line, and the local and distributed global controllers.

By applying Kirchhoff's Current Law (KCL) and Kirchhoff's Voltage Law (KVL) at  $PCC_i$  on the DG side, we get the following equations for  $\Sigma_i^{DG}$ ,  $i \in \mathbb{N}_N$ :

$$\Sigma_i^{DG} : \begin{cases} C_{ti} \frac{dV_i}{dt} = I_{ti} - I_{Li}(V_i) - I_i + w_{vi}(t), \\ L_{ti} \frac{dI_{ti}}{dt} = -V_i - R_{ti}I_{ti} + V_{ti} + w_{ci}(t), \end{cases} \quad (8)$$

where the parameters  $R_{ti}$ ,  $L_{ti}$ , and  $C_{ti}$  represent the internal resistance, internal inductance, and filter capacitance of  $\Sigma_i^{DG}$ , respectively. The state variables are selected as  $V_i$  and  $I_{ti}$ , where  $V_i$  is the  $PCC_i$  voltage and  $I_{ti}$  is the internal current. Moreover,  $V_{ti}$  is the input command signal applied to the VSC,  $I_{Li}(V_i)$  is the load current, and  $I_i$  is the total current injected to the DC MG by  $\Sigma_i^{DG}$ . Without loss of generality,  $w_{vi}(t)$  and  $w_{ci}(t)$  represent unknown bounded external zero-mean noise disturbances affecting the voltage and current dynamics, respectively, where  $|w_{vi}(t)| \leq \delta_{vi}$  and  $|w_{ci}(t)| \leq \delta_{ci}$  ( $\delta_{vi}$  and  $\delta_{ci}$  are known positive constants).

Note that  $V_{ti}$ ,  $I_{Li}(V_i)$ , and  $I_i$  are respectively determined by the controllers, loads, and lines at  $\Sigma_i^{DG}$ . The total line current  $I_i$  is given by

$$I_i = \sum_{l \in \mathcal{E}_i} \mathcal{B}_{il} I_l, \quad (9)$$

where  $I_l, l \in \mathcal{E}_i$  are line currents.

### C. Dynamic Model of a Transmission Line

Each transmission line is modeled using the  $\pi$ -equivalent representation, where we assume that the line capacitances are consolidated with the capacitances of the DG filters. Consequently, as shown in Fig. 2, the power line  $\Sigma_l^{line}$  can be represented as an RL circuit with resistance  $R_l$  and inductance  $L_l$ . By applying KVL to  $\Sigma_l^{line}$ , we obtain:

$$\Sigma_l^{line} : L_l \frac{dI_l}{dt} = -R_l I_l + \bar{u}_l + \bar{w}_l(t), \quad (10)$$

where  $I_l$  is the line current state and  $\bar{u}_l = V_i - V_j = \sum_{i \in \mathcal{E}_l} \mathcal{B}_{il} V_i$ , and  $\bar{w}_l(t)$  represents the unknown bounded external disturbance that affects the line resistance, defined as  $\bar{w}_l(t) = -\Delta R_l(t) I_l$ , where  $|\bar{w}_l(t)| \leq \delta_l$  ( $\delta_l$  is a known positive constant). This disturbance term captures the time-varying uncertainty in line resistance.

### D. Dynamic Model of a Load

Recall that  $I_{Li}(V_i)$  in (8) and Fig. 2 is the current flowing through the load at  $\Sigma_i^{DG}$ ,  $i \in \mathbb{N}_N$ . The exact form of  $I_{Li}(V_i)$

depends on the type of load. In the most general case [20], the load can be thought of as a "ZIP" load where  $I_{Li}(V_i)$  takes the form:

$$I_{Li}(V_i) = I_{Li}^Z(V_i) + I_{Li}^I(V_i) + I_{Li}^P(V_i). \quad (11)$$

Here, the ZIP load's components are: (i) a constant impedance load:  $I_{Li}^Z(V_i) = Y_{Li} V_i$ , where  $Y_{Li} = 1/R_{Li}$  is the conductance of the load, (ii) a constant current load:  $I_{Li}^I(V_i) = \bar{I}_{Li}$  where  $\bar{I}_{Li}$  is the current demand of the load, and (iii) a constant power load:  $I_{Li}^P(V_i) = V_i^{-1} P_{Li}$ , where  $P_{Li}$  represents the power demand of the load.

## IV. PROPOSED CONTROLLER

The control objectives in DC MGs are achieved through the complementary action of local and distributed controllers. The primary aim of local and global controllers is to ensure that the voltage  $PCC_i$  closely follows a specified reference voltage  $V_{ri}$  while achieving proportional current sharing among DG. The local controller at each  $\Sigma_i^{DG}$  is primarily responsible for voltage restoration, where at each  $\Sigma_i^{DG}$ ,  $i \in \mathbb{N}_N$ , we employ a PI controller for voltage regulation. Furthermore, we provide a consensus-based distributed controller to ensure proper current sharing across the MG.

### A. Local Voltage Controller

At each  $\Sigma_i^{DG}$ ,  $i \in \mathbb{N}_N$ , to effectively track the assigned reference voltage  $V_{ri}(t)$ , it is imperative to ensure that the error  $e_i(t) \triangleq V_i(t) - V_{ri}(t)$  converges to zero, i.e.  $\lim_{t \rightarrow \infty} (V_i(t) - V_{ri}(t)) = 0$ , which guarantees that the voltage at each  $\Sigma_i^{DG}$  converges to its reference value. To this end, motivated by [21], we first include each  $\Sigma_i^{DG}$ ,  $i \in \mathbb{N}_N$  with an integrator state  $v_i$  (i.e.  $v_i(t) = \int (V_i(t) - V_{ri}(t)) dt$ ) (see Fig. 2) that follows the dynamics

$$\frac{dv_i}{dt} = e_i(t) = V_i(t) - V_{ri}. \quad (12)$$

Then,  $\Sigma_i^{DG}$  is equipped with a local state feedback controller

$$u_{iL}(t) \triangleq k_{i0}^P (V_i - V_{ri}) + k_{i0}^I v_i(t) = K_{i0} x_i(t) - k_{i0}^P V_{ri}, \quad (13)$$

where  $x_i \triangleq [V_i \ I_{ti} \ v_i]^T \in \mathbb{R}^3$  denotes the augmented state of  $\Sigma_i^{DG}$  and  $K_{i0} = [k_{i0}^P \ 0 \ k_{i0}^I] \in \mathbb{R}^{1 \times 3}$  where  $K_{i0}$  is the local controller gain.

### B. Distributed Global Controller

The local controller alone does not guarantee global stability in the presence of other interconnected DGs.

For current sharing, which the distributed controller manages, the objective is to achieve proportional power sharing

$$\begin{bmatrix} \mathbf{X}_p^{11} & \mathbf{0} & & L_{uy} & & L_{u\bar{y}} \\ \mathbf{0} & \bar{\mathbf{X}}_p^{11} & & L_{\bar{u}y} & & L_{\bar{u}\bar{y}} \\ L_{uy}^\top & L_{\bar{u}y}^\top & -L_{uy}^\top \mathbf{X}^{12} - \bar{\mathbf{X}}^{21} L_{uy} - \bar{\mathbf{X}}_p^{22} & & -\mathbf{X}^{21} L_{u\bar{y}} - L_{\bar{u}\bar{y}}^\top \bar{\mathbf{X}}^{12} & \\ L_{u\bar{y}}^\top & L_{\bar{u}\bar{y}}^\top & -L_{u\bar{y}}^\top \mathbf{X}^{12} - \bar{\mathbf{X}}^{21} L_{u\bar{y}} & & -L_{\bar{u}\bar{y}}^\top \bar{\mathbf{X}}^{12} - \bar{\mathbf{X}}^{21} L_{\bar{u}\bar{y}} - \bar{\mathbf{X}}_p^{22} & \end{bmatrix} > 0 \quad (5)$$

$$\begin{bmatrix} \mathbf{X}_p^{11} & \mathbf{0} & \mathbf{0} & & L_{uy} & & L_{uw} \\ \mathbf{0} & \bar{\mathbf{X}}_p^{11} & \mathbf{0} & & L_{\bar{u}y} & & L_{\bar{u}w} \\ \mathbf{0} & \mathbf{0} & -\mathbf{Y}^{22} & & -\mathbf{Y}^{22} M_{z\bar{y}} & & \mathbf{Y}^{22} M_{zw} \\ L_{uy}^\top & L_{\bar{u}y}^\top & -M_{zy}^\top \mathbf{Y}^{22} & -L_{uy}^\top \mathbf{X}^{12} - \bar{\mathbf{X}}^{21} L_{uy} - \bar{\mathbf{X}}_p^{22} & & -\mathbf{X}^{21} L_{u\bar{y}} - L_{\bar{u}\bar{y}}^\top \bar{\mathbf{X}}^{12} & -\mathbf{X}^{21} L_{uw} + M_{zy}^\top \mathbf{Y}^{21} \\ L_{u\bar{y}}^\top & L_{\bar{u}\bar{y}}^\top & -M_{z\bar{y}}^\top \mathbf{Y}^{22} & -L_{u\bar{y}}^\top \mathbf{X}^{12} - \bar{\mathbf{X}}^{21} L_{u\bar{y}} & & -(L_{\bar{u}\bar{y}}^\top \bar{\mathbf{X}}^{12} + \bar{\mathbf{X}}^{21} L_{\bar{u}\bar{y}} + \bar{\mathbf{X}}_p^{22}) & -\bar{\mathbf{X}}^{21} L_{\bar{u}w} + M_{z\bar{y}}^\top \mathbf{Y}^{21} \\ L_{uw}^\top & L_{\bar{u}w}^\top & -M_{zw}^\top \mathbf{Y}^{22} & -L_{uw}^\top \mathbf{X}^{12} + \mathbf{Y}^{12} M_{zy} & & -L_{\bar{u}w}^\top \bar{\mathbf{X}}^{12} + \mathbf{Y}^{12} M_{z\bar{y}} & M_{zw}^\top \mathbf{Y}^{21} + \mathbf{Y}^{12} M_{zw} + \mathbf{Y}^{11} \end{bmatrix} > 0 \quad (7)$$



inputs and affects on performance outputs.

To this end, we first use (18) and (16) to state the closed-loop dynamics of  $\Sigma_i^{DG}$  as (see also Co. 1)

$$\dot{x}_i = (A_i + B_i K_{i0})x_i + \tilde{\eta}_i, \quad (23)$$

where  $\tilde{u}_i$  in (23) can be stated as

$$\tilde{\eta}_i = E_i w_i(t) + \sum_{l \in \mathcal{E}_i} \bar{C}_{il} \bar{x}_l + \sum_{j \in \bar{\mathcal{F}}_i^-} K_{ij} x_j + \theta_i, \quad (24)$$

where  $\bar{C}_{il} \triangleq -C_{ti}^{-1} [\mathcal{B}_{il} \ 0 \ 0]^\top, \forall l \in \mathcal{E}_i$ , and the remaining can be defined as  $\theta_i \triangleq E_i \bar{w}_i + B_i u_{iS} - B_i k_{i0}^P V_{ri}$ . To capture the distributed current sharing objective through the communication network, we define the coupling gain matrix:

$$K_{ij} \triangleq \frac{1}{L_{ti}} \begin{bmatrix} 0 & 0 & 0 \\ 0 & k_{ij}^I & 0 \\ 0 & 0 & 0 \end{bmatrix}, \quad \forall j \in \bar{\mathcal{F}}_i^-. \quad (25)$$

The structure of  $K_{ij}$  reflects that only the current states are coupled through the communication network, where  $k_{ij}^I$  represents the consensus gain between  $\Sigma_i^{DG}$  and  $\Sigma_j^{DG}$ . The zero elements ensure that voltage and integrator states remain decoupled in the distributed control implementation.

By vectorizing (24) over all  $i \in \mathbb{N}_N$ , we get

$$\tilde{\eta} \triangleq Ew + \bar{C}\bar{x} + Kx + \theta, \quad (26)$$

where  $\tilde{\eta} \triangleq [\tilde{\eta}_i]_{i \in \mathbb{N}_N}$  represents the effective input vector to the DGs,  $\bar{C} \triangleq [\bar{C}_{il}]_{i \in \mathbb{N}_N, l \in \mathbb{N}_L}$  and  $K \triangleq [K_{ij}]_{i, j \in \mathbb{N}_N}$ ,  $E \triangleq \text{diag}([E_i]_{i \in \mathbb{N}_N})$  is the vector of DG disturbances, and  $\theta \triangleq [\theta_i]_{i \in \mathbb{N}_N}$  represents a constant input vector applied in DGs.

**Remark 4:** The block matrices  $K$  and  $\bar{C}$  in (26) are indicative of the communication and physical topologies of the DC MG, respectively. In particular, the  $(i, j)$ <sup>th</sup> block in  $K$ , i.e.,  $K_{ij}$  indicates a communication link from  $\Sigma_j^{DG}$  to  $\Sigma_i^{DG}$ . Similarly,  $(i, l)$ <sup>th</sup> block in  $\bar{C}$  indicates a physical link from  $\Sigma_i^{DG}$  and  $\Sigma_l^{Line}$ .

Similarly to DGs, we use the closed-loop dynamics of  $\Sigma_l^{Line}$ , using (21)

$$\dot{\bar{x}}_l = \bar{A}_l \bar{x}_l + \tilde{\eta}_l, \quad (27)$$

which  $\tilde{u}$  can be stated as

$$\tilde{\eta}_l = \sum_{i \in \mathcal{E}_l} C_{il} x_i + \bar{E}_l \bar{w}_l(t), \quad (28)$$

with  $C_{il} \triangleq [\mathcal{B}_{il} \ 0 \ 0], \forall l \in \mathcal{E}_i$ . Note also that  $C_{il} = -C_{ti} \bar{C}_{il}^\top$ . By vectorizing (28) over all  $l \in \mathbb{N}_L$ , we get

$$\tilde{\eta} = Cx + \bar{E}\bar{w}, \quad (29)$$

where  $\tilde{\eta} \triangleq [\tilde{\eta}_l]_{l \in \mathbb{N}_L}$  represents the effective input vector to the lines,  $C \triangleq [C_{il}]_{l \in \mathbb{N}_L, i \in \mathbb{N}_N}$ ,  $\bar{E} \triangleq \text{diag}([\bar{E}_l]_{l \in \mathbb{N}_L})$ , and  $\bar{w} \triangleq [\bar{w}_l]_{l \in \mathbb{N}_L}$  is the vector of line disturbances. Note also that  $C = -\bar{C}^\top C_t$  where  $C_t \triangleq \text{diag}([C_{ti} \mathbf{I}_3]_{i \in \mathbb{N}_N})$ .

Finally, using (26) and (29), we can identify the interconnection relationship:  $[\tilde{\eta}^\top \ \tilde{\eta}^\top]^\top = M[x^\top \ \bar{x}^\top \ w^\top \ \bar{w}^\top]^\top$ , where the interconnection matrix  $M$  takes the form:

$$M \triangleq \begin{bmatrix} M_{\tilde{\eta}x} & M_{\tilde{\eta}\bar{x}} & M_{\tilde{\eta}w} & M_{\tilde{\eta}\bar{w}} \\ M_{\tilde{\eta}\bar{x}} & M_{\tilde{\eta}\bar{w}} & M_{\tilde{\eta}w} & M_{\tilde{\eta}\bar{w}} \end{bmatrix} \equiv \begin{bmatrix} K & \bar{C} & E & \mathbf{0} \\ C & \mathbf{0} & \mathbf{0} & \bar{E} \end{bmatrix}. \quad (30)$$

When the physical topology  $\mathcal{G}^p$  is predefined, so are the block matrices  $\bar{C}$  and  $C$  (recall  $C = -\bar{C}^\top C_t$ ). This leaves only the block matrix  $K$  inside the block matrix  $M$  as a

tunable quantity to optimize the desired input-output (from  $w$  to  $z$ ) properties of the closed-loop DC MG system. Note that synthesizing  $K$  simultaneously determines the distributed global controllers and the communication topology  $\mathcal{G}^c$ . In the following section, we provide a systematic dissipativity-based approach to synthesize this block matrix  $K$ .

## V. STABILITY ANALYSIS OF DC MG

The fundamental challenge in DC MG control stems from the inherent conflict between voltage regulation and current sharing objectives. Line impedance variations and load uncertainties often create a trade-off between these goals. Our proposed hierarchical structure resolves this conflict by separating the objectives into distinct but coordinated control layers.

### A. Equilibrium Point Analysis of the DC MG

To express these equilibrium conditions in vector form, we define time-varying parameters:  $V_E \triangleq [V_{iE}]_{i \in \mathbb{N}_N} \in \mathbb{R}^{N \times 1}$ ,  $I_{tE} \triangleq [I_{tiE}]_{i \in \mathbb{N}_N} \in \mathbb{R}^{N \times 1}$ ,  $u_E \triangleq [u_{iE}]_{i \in \mathbb{N}_N} \in \mathbb{R}^{N \times 1}$ ,  $\bar{I}_E \triangleq [\bar{I}_{lE}]_{l \in \mathbb{N}_L} \in \mathbb{R}^{L \times 1}$ , and constant system parameters:  $C_t \triangleq \text{diag}([C_{ti}]_{i \in \mathbb{N}_N}) \in \mathbb{R}^{N \times N}$ ,  $Y_L \triangleq \text{diag}([Y_{lE}]_{l \in \mathbb{N}_L}) \in \mathbb{R}^{N \times N}$ ,  $L_t \triangleq \text{diag}([L_{ti}]_{i \in \mathbb{N}_N}) \in \mathbb{R}^{N \times N}$ ,  $R_t \triangleq \text{diag}([R_{ti}]_{i \in \mathbb{N}_N}) \in \mathbb{R}^{N \times N}$ ,  $\bar{I}_L \triangleq \text{diag}([\bar{I}_{lE}]_{l \in \mathbb{N}_L}) \in \mathbb{R}^{N \times N}$ ,  $V_r \triangleq [V_{ri}]_{i \in \mathbb{N}_N} \in \mathbb{R}^{N \times 1}$ ,  $R \triangleq \text{diag}([R_{li}]_{l \in \mathbb{N}_L}) \in \mathbb{R}^{L \times L}$ ,  $\mathcal{B} \triangleq [\mathcal{B}_{il}]_{i \in \mathbb{N}_N, l \in \mathbb{N}_L} \in \mathbb{R}^{N \times L}$ .

**Lemma 1:** Assuming all zero mean disturbance components to be zero, i.e.,  $w_i(t) = 0, \forall i \in \mathbb{N}_N$  and  $\bar{w}_l(t) = 0, \forall l \in \mathbb{N}_L$ , for a given reference voltage vector  $V_r$ , under a fixed control input vector  $u_E$  defined as

$$u_E \triangleq [\mathbf{I} + R_t(\mathcal{B}R^{-1}\mathcal{B}^\top + Y_L)]V_r + R_t \bar{I}_L, \quad (31)$$

there exists an equilibrium point for the DC MG characterized by the equilibrium DG voltage, DG current, and line current vectors, respectively, given by:

$$\begin{aligned} V_E &= V_r, \\ I_{tE} &= (\mathcal{B}R^{-1}\mathcal{B}^\top + Y_L)V_r + \bar{I}_L, \\ \bar{I}_E &= R^{-1}\mathcal{B}^\top V_r. \end{aligned} \quad (32)$$

**Proof:** The equilibrium state of the closed-loop dynamic  $\Sigma_i^{DG}$  (18) can be written as:

$$\dot{x}_{iE}(t) = A_i x_{iE}(t) + B_i u_{iE}(t) + E_i d_{iE}(t) + \xi_{iE}(t), \quad (33)$$

where  $x_{iE} = [V_{iE} \ I_{tiE} \ v_{iE}]^\top$  represents the equilibrium state of DG. The  $V_{iE}$ ,  $V_{ri}$ ,  $I_{tiE}$ ,  $v_{iE}$ ,  $u_{iE}$ ,  $w_{iE}$ , and  $\xi_{iE}$  represent the equilibrium values of voltage, reference voltage, current, integrator states, control input, disturbance, and interconnection term, respectively.

An equilibrium state of the closed-loop system (33) can be obtained by setting  $\dot{x} = 0$ :

$$\begin{bmatrix} -\frac{Y_{li}}{C_{ti}} & -\frac{1}{C_{ti}} & 0 \\ -\frac{1}{L_{ti}} & -\frac{R_{ti}}{L_{ti}} & 0 \\ 1 & 0 & 0 \end{bmatrix} \begin{bmatrix} V_{iE} \\ I_{tiE} \\ v_{iE} \end{bmatrix} + \begin{bmatrix} 0 \\ \frac{1}{L_{ti}} \\ 0 \end{bmatrix} u_{iE} + E_i \bar{w}_i + \xi_{iE} = 0 \quad (34)$$

Similarly, the equilibrium state of the closed-loop dynamic  $\Sigma_l^{Line}$  (21) can be written as:

$$\dot{\bar{x}}_l(t) = \bar{A}_l \bar{x}_l(t) + \bar{B}_l \bar{u}_l + \bar{E}_l \bar{w}_l(t), \quad (35)$$

where  $\bar{x}_{lE} \triangleq \bar{I}_{lE}$  represents the equilibrium state of line. The  $\bar{u}_{lE}$  and  $\bar{w}_{lE}$ , respectively, represent the equilibrium values of control input and disturbance of lines.

An equilibrium state of line dynamics can be obtained by setting  $\dot{\bar{x}} = 0$ :

$$-\frac{R_l}{L_l}\bar{I}_{lE} + \frac{1}{L_l}\sum_{i \in \mathcal{E}_l}\mathcal{B}_{il}V_{iE} = 0. \quad (36)$$

where  $\bar{I}_{lE} \in \mathbb{R}^L$  represents the equilibrium value of line current.

From the voltage dynamics (first row):

$$-\frac{Y_{Li}}{C_{ti}}V_{iE} + \frac{1}{C_{ti}}I_{tiE} - \frac{1}{C_{ti}}\bar{I}_{Li} - \frac{1}{C_{ti}}\sum_{l \in \mathcal{E}_i}\mathcal{B}_{il}\bar{I}_{lE} = 0. \quad (37)$$

From the current dynamics (second row):

$$-\frac{1}{L_{ti}}V_{iE} - \frac{R_{ti}}{L_{ti}}I_{tiE} + \frac{1}{L_{ti}}u_{iE} = 0. \quad (38)$$

From the integrator dynamics (third row):

$$V_{iE} - V_{ri} = 0. \quad (39)$$

From these equations, we obtain the following relationships.

From the integrator dynamics (39):

$$V_{iE} = V_{ri}. \quad (40)$$

From the current dynamics (38):

$$u_{iE} = V_{iE} + R_{ti}I_{tiE}. \quad (41)$$

From the line dynamics (36):

$$\bar{I}_{lE} = \frac{1}{R_l}\sum_{i \in \mathcal{E}_l}\mathcal{B}_{il}V_{iE} = \frac{1}{R_l}\sum_{j \in \mathcal{E}_l}\mathcal{B}_{jl}V_{jE}. \quad (42)$$

Applying the voltage equilibrium (40) and line current (42) relationships to the voltage dynamics (37):

$$-Y_{Li}V_{ri} + I_{tiE} - \sum_{l \in \mathcal{E}_i}\mathcal{B}_{il}\frac{1}{R_l}\sum_{j \in \mathcal{E}_l}\mathcal{B}_{jl}V_{rj} - \bar{I}_{Li} = 0. \quad (43)$$

The control equilibrium equation (41) becomes:

$$u_E = V_r + R_t I_{tE}.$$

Vectorizing the voltage dynamics equation:

$$-Y_L V_r + I_{tE} - \mathcal{B}R^{-1}\mathcal{B}^\top V_r - \bar{I}_L = 0,$$

therefore:

$$I_{tE} = (\mathcal{B}R^{-1}\mathcal{B}^\top + Y_L)V_r + \bar{I}_L.$$

The control input can then be expressed as:

$$\begin{aligned} u_E &= V_r + R_t I_{tE}, \\ &= V_r + R_t(\mathcal{B}R^{-1}\mathcal{B}^\top + Y_L)V_r + R_t \bar{I}_L, \\ &= [\mathbf{I} + R_t(\mathcal{B}R^{-1}\mathcal{B}^\top + Y_L)]V_r + R_t \bar{I}_L. \end{aligned}$$

For the line dynamics:

$$\bar{I}_E = R^{-1}\mathcal{B}^\top V_r. \quad \blacksquare$$

**Remark 5:** For any given  $V_r$ , all equilibrium variables ( $V_E$ ,  $I_{tE}$ ,  $u_E$ , and  $\bar{I}_E$ ) characterized in Lm. 1 are uniquely determined through linear relationships involving system parameters ( $R_t$ ,  $R$ ,  $Y_L$ ,  $\mathcal{B}$ ) and the constant load current vector  $\bar{I}_L$ . The uniqueness is guaranteed by the diagonal structure of matrices  $\mathcal{B}$ ,  $R$ , and  $Y_L$  with fixed positive elements in the equilibrium equations (32) of Lm. 1, ensuring a unique mapping from  $V_r$  to all equilibrium variables.

**Remark 6:** The proportional current sharing among DG units is governed by one equation. The per-DG current sharing relationship:

$$\frac{I_{tiE}}{P_{ni}} = I_s \iff I_{tiE} = P_{ni}I_s, \quad \forall i \in \mathbb{N}_N, \quad (44)$$

where  $P_{ni}$  is the power rating of  $\Sigma_i^{DG}$  and  $I_s$  is a scalar design variable shared across the entire DC MG. This can be expressed in vectorized form as:

$$I_{tE} = P_n \mathbf{1}_N I_s, \quad (45)$$

where  $\mathbf{1}_N = [1, 1, \dots, 1]^\top \in \mathbb{R}^N$  and  $P_n \triangleq \text{diag}([P_{ni}]_{i \in \mathbb{N}_N})$ . This relationship ensures that at equilibrium, the DG currents are distributed proportionally to their power ratings  $P_n$ . The variable  $I_s$  serves as a global current sharing index that quantifies the power contribution from each  $\Sigma_i^{DG}$  relative to its rated capacity, while maintaining the voltage regulation objective. Therefore, with respect to (44), the steady-state control input  $u_{iS}$  determined from (41), can be written as:

$$u_{iS} = V_{ri} + R_{ti}P_{ni}I_s \quad (46)$$

In conclusion, using Lm. 1 and Rm. 6, for the equilibrium of DC MG, we require:

$$\begin{aligned} u_E &= [\mathbf{I} + R_t(\mathcal{B}R^{-1}\mathcal{B}^\top + Y_L)]V_r + R_t \bar{I}_L \\ V_E &= V_r \\ I_{tE} &= (\mathcal{B}R^{-1}\mathcal{B}^\top + Y_L)V_r + \bar{I}_L = P_n \mathbf{1}_N I_s \\ \bar{I}_E &= R^{-1}\mathcal{B}^\top V_r \end{aligned} \quad (47)$$

These equations establish the existence of an equilibrium point.

**Theorem 1:** The current sharing objective imposes additional constraints on the selection of the reference voltage vector  $V_r$  and sharing coefficient  $I_s$ :

$$\begin{aligned} \text{Find:} \quad & \alpha_V \|V_r - \bar{V}_r\|^2 + \alpha_I I_s \\ \text{Sub. to:} \quad & P_n \mathbf{1}_N I_s - (\mathcal{B}R^{-1}\mathcal{B}^\top + Y_L)V_r = \bar{I}_L, \\ & V_{\min} \leq V_r \leq V_{\max}, \\ & 0 \leq I_s \leq 1, \end{aligned} \quad (48)$$

where  $V_{\min}$  and  $V_{\max}$  represent the acceptable voltage bounds for the DC MG,  $\alpha_V > 0$  is the voltage reference tracking weight, and  $\alpha_I > 0$  is the current sharing weight.

This formulation ensures proper system operation through multiple aspects. The equality constraint guarantees that the current sharing objective is achieved across all DG units. The voltage bounds maintain system operation within safe and efficient limits through the inequality constraints on  $V_r$ . Furthermore, the constraint on  $I_s$  ensures the sharing coefficient remains properly normalized for practical implementation. The feasible solution set of this LMI problem provides valid combinations of  $V_r$  and  $I_s$  that simultaneously satisfy both voltage regulation and current sharing objectives while respecting system constraints.



## B. Error Dynamics Networked System

The network system representation described in Sec. IV-D can be simplified by considering the error system dynamics without exogenous disturbances. This simplified structure focuses solely on the coupling between DG error subsystems and line error subsystems.

We first define error variables that capture deviations from the desired equilibrium:

$$\tilde{V}_i = V_i - V_{iE} = V_i - V_{ri} \quad (49a)$$

$$\tilde{I}_{ti} = I_{ti} - I_{tiE} = I_{ti} - P_{ni}I_s \quad (49b)$$

$$\tilde{v}_i = v_i - v_{iE} \quad (49c)$$

$$\tilde{I}_l = I_l - \bar{I}_{lE} = I_l - \frac{1}{R_l} \sum_{i \in \mathcal{E}_l} \mathcal{B}_{il} V_{ri} \quad (49d)$$

Consider the dynamical system described by equations 37-39, and propose a hierarchical control strategy  $u_i(t)$  of the form defined in (16). The error dynamics can then be derived as follows. The voltage error dynamic can be derived using (17a) and (49a):

$$\begin{aligned} \dot{\tilde{V}}_i &= -\frac{Y_{Li}}{C_{ti}}(\tilde{V}_i + V_{ri}) + \frac{1}{C_{ti}}(\tilde{I}_{ti} + P_{ni}I_s) \\ &\quad - \frac{1}{C_{ti}}\bar{I}_{Li} - \frac{1}{C_{ti}} \sum_{l \in \mathcal{E}_i} \mathcal{B}_{il}(\tilde{I}_l + \frac{1}{R_l} \sum_{j \in \mathcal{E}_l} \mathcal{B}_{jl} V_{rj}) \\ &= \frac{1}{C_{ti}}\phi_V + \frac{1}{C_{ti}}\psi_V, \end{aligned} \quad (50)$$

where

$$\phi_V = -Y_{Li}\tilde{V}_i + \tilde{I}_{ti} - \sum_{l \in \mathcal{E}_i} \mathcal{B}_{il}\tilde{I}_l, \quad (51a)$$

$$\psi_V = -Y_{Li}V_{ri} + P_{ni}I_s - \bar{I}_{Li} - \sum_{l \in \mathcal{E}_i} \frac{\mathcal{B}_{il}}{R_l} \sum_{j \in \mathcal{E}_l} \mathcal{B}_{jl} V_{rj}. \quad (51b)$$

The current error dynamic can be achieved by using (17b) and (49b):

$$\begin{aligned} \dot{\tilde{I}}_{ti} &= -\frac{1}{L_{ti}}(\tilde{V}_i + V_{ri}) - \frac{R_{ti}}{L_{ti}}(\tilde{I}_{ti} + P_{ni}I_s) \\ &\quad + \frac{1}{L_{ti}}(u_{iS} + k_{i0}^P \tilde{V}_i + k_{i0}^I \tilde{v}_i + \sum_{j \in \mathcal{F}_i^-} k_{ij}(\frac{\tilde{I}_{ti}}{P_{ni}} - \frac{\tilde{I}_{tj}}{P_{nj}})), \\ &= \frac{1}{L_{ti}}\phi_I + \frac{1}{L_{ti}}\psi_I, \end{aligned} \quad (52)$$

where

$$\phi_I = -\tilde{V}_i - R_{ti}\tilde{I}_{ti} + k_{i0}^P \tilde{V}_i + k_{i0}^I \tilde{v}_i + \sum_{j \in \mathcal{F}_i^-} k_{ij}(\frac{\tilde{I}_{ti}}{P_{ni}} - \frac{\tilde{I}_{tj}}{P_{nj}}), \quad (53a)$$

$$\psi_I = -V_{ri} - R_{ti}P_{ni}I_s + u_{iS}. \quad (53b)$$

The integral error dynamics can be achieved by using (17c) and (49c):

$$\dot{\tilde{v}}_i = \tilde{V}_i \quad (54)$$

For the analysis of error dynamics, we set  $w_i(t) = 0, \forall i \in \mathbb{N}_N$  and  $\bar{w}_l(t) = 0, \forall l \in \mathbb{N}_L$ . The known disturbance components  $\bar{w}_i(t)$  are automatically eliminated by equilibrium analysis. Based on (43) and using (44), the term (51b) can

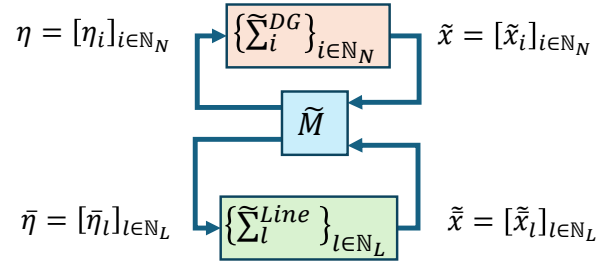


Fig. 4. DC MG error dynamics as a networked system configuration.

be canceled. Furthermore, based on (46), the term (53b) can be canceled due to equilibrium analysis.

DG and line error dynamics can be represented as two interconnected subsystems through a static interconnection matrix  $\tilde{M}$ , as shown in Fig. 4. The network error system is discussed without disturbances and performance outputs by comparing Fig. 4 with Fig. 3.

For each DG error subsystem  $\tilde{\Sigma}_i^{DG}, i \in \mathbb{N}_N$ , we have error state vector  $\tilde{x}_i = [\tilde{V}_i, \tilde{I}_{ti}, \tilde{v}_i]^\top$ . The DG error dynamics can be written in form of

$$\dot{\tilde{x}}_i = A_i \tilde{x}_i + u_i, \quad (55)$$

where  $\eta_i$  represents the interconnection input combining the effects of both line currents and other DG states:

$$u_i = \begin{bmatrix} \sum_{l \in \mathcal{E}_i} \bar{C}_{il} \tilde{x}_l \\ \sum_{j \in \mathcal{F}_i^-} K_{ij} x_j \\ 0 \end{bmatrix} \quad (56)$$

For each transmission line error subsystem  $\tilde{\Sigma}_l^{Line}, l \in \mathbb{N}_L$ :

$$\dot{\tilde{x}}_l = \bar{A}_l \tilde{x}_l + \bar{u}_l, \quad (57)$$

where  $\bar{\eta}$  represents the line interconnection input influenced by DG voltages:

$$\bar{u}_l = \sum_{i \in \mathcal{E}_l} B_{il} \tilde{V}_i \quad (58)$$

Let us define  $u \triangleq [u_i]_{i \in \mathbb{N}_N}$  and  $\bar{u} \triangleq [\bar{u}_l]_{l \in \mathbb{N}_L}$  respectively as control inputs of DGs and lines,  $\tilde{x} \triangleq [\tilde{x}_i]_{i \in \mathbb{N}_N}$  and  $\tilde{x} \triangleq [\tilde{x}_l]_{l \in \mathbb{N}_L}$  respectively as the full state of DGs and lines of the DC MG.

To identify the specific structure of the interconnection matrix  $\tilde{M}$  in Fig. 4, we need to closely observe how the error dynamics of DGs and lines are interconnected. We can identify the interconnection  $[u^\top \ \bar{u}^\top]^\top = \tilde{M} [\tilde{x}^\top \ \tilde{x}^\top]^\top$ , where the interconnection matrix  $\tilde{M}$  takes the form:

$$\tilde{M} \triangleq \begin{bmatrix} M_{u\tilde{x}} & M_{\bar{u}\tilde{x}} \\ M_{\tilde{x}u} & M_{\tilde{x}\bar{u}} \end{bmatrix} \equiv \begin{bmatrix} K & \bar{C} \\ C & \mathbf{0} \end{bmatrix} \quad (59)$$

where  $K \triangleq [K_{ij}]_{i,j \in \mathbb{N}_N}$  with  $K_{ij}$  defined in (25),  $\bar{C} \triangleq [\bar{C}_{il}]_{i \in \mathbb{N}_N, l \in \mathbb{N}_L}$  with  $\bar{C}_{il} \triangleq -C_{ti}^{-1} [\mathcal{B}_{il} \ 0 \ 0]^\top, \forall l \in \mathcal{E}_i$  and  $C \triangleq [C_{il}]_{l \in \mathbb{N}_L, i \in \mathbb{N}_N}$  with  $C_{il} \triangleq [\mathcal{B}_{il} \ 0 \ 0], \forall l \in \mathcal{E}_i$ .

## C. Stability Analysis of the DC MG

Consider the error dynamic subsystem  $\tilde{\Sigma}_i^{DG}, i \in \mathbb{N}_N$  (23), which is assumed to be  $X_i$ -EID with

$$X_i = \begin{bmatrix} X_i^{11} & X_i^{12} \\ X_i^{21} & X_i^{22} \end{bmatrix} \triangleq \begin{bmatrix} -\nu_i \mathbf{I} & \frac{1}{2} \mathbf{I} \\ \frac{1}{2} \mathbf{I} & -\rho_i \mathbf{I} \end{bmatrix}, \quad (60)$$

where  $\rho_i$  and  $\nu_i$  are the error passivity indices of  $\tilde{\Sigma}_i^{DG}$ , i.e., each  $\tilde{\Sigma}_i^{DG}, i \in \mathbb{N}_N$  is assumed to be IF-OfP( $\nu_i, \rho_i$ ).



Similarly, consider the error dynamic subsystem  $\tilde{\Sigma}_l^{Line}, l \in \mathbb{N}_L$  (21), which is assumed to be  $X_l$ -EID with

$$\bar{X}_l = \begin{bmatrix} \bar{X}_l^{11} & \bar{X}_l^{12} \\ \bar{X}_l^{21} & \bar{X}_l^{22} \end{bmatrix} \triangleq \begin{bmatrix} -\bar{\nu}_l \mathbf{I} & \frac{1}{2} \mathbf{I} \\ \frac{1}{2} \mathbf{I} & -\bar{\rho}_l \mathbf{I} \end{bmatrix}, \quad (61)$$

where  $\bar{\rho}_l$  and  $\bar{\nu}_l$  are the error passivity indices of  $\tilde{\Sigma}_l^{Line}$ .

Unlike the passivity properties of DGs, as shown in the following lemma, we can directly comment on the passivity properties of lines using their dynamics (21) in Prop. 1 (as stated earlier, all proofs can be found in [22]).

**Lemma 2:** For each line  $\tilde{\Sigma}_l^{Line}, l \in \mathbb{N}_L$  (21), its passivity indices  $\bar{\nu}_l, \bar{\rho}_l$  assumed in (61) are such that the LMI problem:

$$\text{Find: } \bar{P}_l, \bar{\nu}_l, \bar{\rho}_l$$

$$\text{Sub. to: } \bar{P}_l > 0, \begin{bmatrix} \frac{2\bar{P}_l R_l}{L_l} - \bar{\rho}_l & -\frac{\bar{P}_l}{L_l} + \frac{1}{2} \\ \star & -\bar{\nu}_l \end{bmatrix} \geq 0, \quad (62)$$

is feasible. The maximum feasible values for  $\bar{\nu}_l$  and  $\bar{\rho}_l$  respectively are  $\bar{\nu}_l^{\max} = 0$  and  $\bar{\rho}_l^{\max} = R_l$ , when  $\bar{P}_l = \frac{L_l}{2}$ .

The interconnection matrix  $\tilde{M}$ , particularly its block  $M_{\eta\bar{x}} = K$ , can be synthesized by applying the above error dynamics subsystems to Prop. 2. By synthesizing  $K = [K_{ij}]_{i,j \in \mathbb{N}_N}$ , we can get the condition on the distributed global controller gains  $\{k_{ij}^l : i, j \in \mathbb{N}_N\}$  (25) along with the required communication topology  $\mathcal{G}^c$ . The following theorem formulates this distributed global controller and communication topology co-design problem.

In the following theorem, we demonstrate that the equilibrium states are indeed stable under our proposed control law, thereby justifying their designation as steady states.

**Theorem 2:** For the error system with DG error subsystems having IF-OPF( $\nu_i, \rho_i$ ) properties and line error subsystems having IF-OPF( $\bar{\nu}_l, \bar{\rho}_l$ ), the system is stable and achieves disturbance attenuation by synthesizing the interconnection matrix  $M_{\eta\bar{x}} = K$  (59) via solving the LMI problem:

$$\min_{\substack{Q, \{p_i : i \in \mathbb{N}_N\}, \\ \{\bar{p}_l : l \in \mathbb{N}_L\}}} \sum_{i,j \in \mathbb{N}_N} c_{ij} \|Q_{ij}\|_1, \quad (63)$$

$$\text{Sub. to: } p_i > 0, \forall i \in \mathbb{N}_N, \bar{p}_l > 0, \forall l \in \mathbb{N}_L, \\ \text{and (64),}$$

as  $K = (\mathbf{X}_p^{11})^{-1}Q$ , where  $\mathbf{X}^{12} \triangleq \text{diag}([-\frac{1}{2\nu_i} \mathbf{I}]_{i \in \mathbb{N}_N})$ ,  $\mathbf{X}^{21} \triangleq (\mathbf{X}^{12})^\top$ ,  $\bar{\mathbf{X}}^{12} \triangleq \text{diag}([-\frac{1}{2\bar{\nu}_l} \mathbf{I}]_{l \in \mathbb{N}_L})$ ,  $\bar{\mathbf{X}}^{21} \triangleq (\bar{\mathbf{X}}^{12})^\top$ ,  $\mathbf{X}_p^{11} \triangleq \text{diag}([-p_i \nu_i \mathbf{I}]_{i \in \mathbb{N}_N})$ ,  $\mathbf{X}_p^{22} \triangleq \text{diag}([-p_i \rho_i \mathbf{I}]_{i \in \mathbb{N}_N})$ ,  $\bar{\mathbf{X}}_{\bar{p}}^{11} \triangleq \text{diag}([-\bar{p}_l \bar{\nu}_l \mathbf{I}]_{l \in \mathbb{N}_L})$ , and  $\bar{\mathbf{X}}_{\bar{p}}^{22} \triangleq \text{diag}([-\bar{p}_l \bar{\rho}_l \mathbf{I}]_{l \in \mathbb{N}_L})$ . The coefficient  $c_{ij} > 0, \forall i, j \in \mathbb{N}_N$  is a predefined cost coefficient for communication links.

The feasibility of the global codesign problem for dynamic error subsystems depends on passivity indices  $\{\nu_i, \rho_i\}$  and  $\{\bar{\nu}_l, \bar{\rho}_l\}$  of the DGs and lines, appearing in terms  $\mathbf{X}_p^{11}$ ,  $\mathbf{X}_p^{22}$ ,  $\bar{\mathbf{X}}_{\bar{p}}^{11}$ ,  $\bar{\mathbf{X}}_{\bar{p}}^{22}$ ,  $\mathbf{X}^{12}$ ,  $\mathbf{X}^{21}$ ,  $\bar{\mathbf{X}}^{12}$  and  $\bar{\mathbf{X}}^{21}$  in (64). To enable local controller design and passivity analysis, there must be necessary conditions for error dynamics to ensure feasible global control synthesis as in Th. 2.

$$\begin{bmatrix} \mathbf{X}_p^{11} & \mathbf{0} & Q & \mathbf{X}_p^{11} \bar{C} \\ \mathbf{0} & \bar{\mathbf{X}}_{\bar{p}}^{11} & \bar{\mathbf{X}}_{\bar{p}}^{11} C & \mathbf{0} \\ Q^\top & C^\top \bar{\mathbf{X}}_{\bar{p}}^{11} & -Q^\top \mathbf{X}^{12} - \mathbf{X}^{21} Q - \mathbf{X}_p^{22} & -\mathbf{X}^{21} \mathbf{X}_p^{11} \bar{C} - C^\top \bar{\mathbf{X}}_{\bar{p}}^{11} \bar{\mathbf{X}}^{12} \\ \bar{C}^\top \mathbf{X}_p^{11} & \mathbf{0} & -\bar{C}^\top \mathbf{X}_p^{11} \mathbf{X}^{12} - \bar{\mathbf{X}}^{21} \bar{\mathbf{X}}_{\bar{p}}^{11} C & -\bar{\mathbf{X}}_{\bar{p}}^{22} \end{bmatrix} > 0 \quad (64)$$

**Lemma 3:** For the LMI conditions in (63) in Th. 2 to hold, it is necessary that the error DG and line passivity indices  $\{\nu_i, \rho_i : i \in \mathbb{N}_N\}$  (60) and  $\{\bar{\nu}_l, \bar{\rho}_l : l \in \mathbb{N}_L\}$  (61) are such that the LMI problem:

$$\text{Find: } \{(\nu_i, \rho_i) : i \in \mathbb{N}_N\}, \{(\bar{\nu}_l, \bar{\rho}_l) : l \in \mathbb{N}_L\}$$

$$\text{Sub. to: } p_i > 0, \forall i \in \mathbb{N}_N \text{ and } \bar{p}_l > 0, \forall l \in \mathbb{N}_L \\ \text{and (66),}$$

is feasible.

To enforce the identified necessary LMI conditions in Lm. 3 (65) on error DG and line passivity indices, a relaxed local controller synthesis problem is formulated.

**Theorem 3:** For the error system with DG and line error subsystems having IF-OPF( $\nu_i, \rho_i$ ) (60) and IF-OPF( $\bar{\nu}_l, \bar{\rho}_l$ ) (61) properties, the local controller gains  $\{K_{i0}, i \in \mathbb{N}_N\}$  (13) and error passivity indices can be determined by solving the following LMI problem:

$$\text{Find: } \{(\tilde{K}_{i0}, P_i, \nu_i, \rho_i) : i \in \mathbb{N}_N\}, \{(\bar{P}_l, \bar{\nu}_l, \bar{\rho}_l) : l \in \mathbb{N}_L\}$$

Sub. to:

$$P_i > 0, \begin{bmatrix} \rho_i \mathbf{I} & P_i & \mathbf{0} \\ P_i & -\mathcal{H}(A_i P_i + B_i \tilde{K}_{i0}) & -\mathbf{I} + \frac{1}{2} P_i \\ \mathbf{0} & -\mathbf{I} + \frac{1}{2} P_i & -\nu_i \mathbf{I} \end{bmatrix} > 0, \forall i \in \mathbb{N}_N,$$

$$\bar{P}_l > 0, \begin{bmatrix} \frac{2\bar{P}_l R_l}{L_l} - \bar{\rho}_l & -\frac{\bar{P}_l}{L_l} + \frac{1}{2} \\ \star & -\bar{\nu}_l \end{bmatrix} \geq 0, \forall l \in \mathbb{N}_L,$$

and sub. to the necessary condition in (66),

where  $K_{i0} \triangleq \tilde{K}_{i0} P_i^{-1}$ .

**Remark 7:** The equilibrium analysis assumes that the unknown disturbances  $w_i(t)$  converge to zero in steady state. This is a reasonable assumption for many practical disturbances in DC MGs. However, for persistent unknown disturbances, the control system's ability to reject these disturbances and maintain operation near the desired equilibrium point is analyzed through the dissipativity-based approach in the following sections.

## VI. DISSIPATIVITY-BASED CONTROL AND TOPOLOGY CO-DESIGN

In this section, we first introduce the global control and topology co-design problem for a DC MG with performance and disturbance evaluation of DGs and transmission lines, as illustrated in Fig. 5. Next, necessary prerequisites for subsystem dissipativity properties are given. We then formulate a customized local controller design problem. Finally, the overall control design process is summarized.

For each DG subsystem  $\Sigma_i^{DG}, i \in \mathbb{N}_N$ , we define the performance output as:

$$z_i(t) = H_i x_i(t), \quad (67)$$

where  $H_i = \mathbf{I}$  is the identity matrix. Similarly, for each line subsystem  $\Sigma_l^{Line}, l \in \mathbb{N}_L$ , we define the performance output as:

$$\bar{z}_l(t) = \bar{H}_l \bar{x}_l(t), \quad (68)$$

where  $\bar{H}_l = \mathbf{I}$  is the identity matrix.

Upon vectorizing over all  $i \in \mathbb{N}_N$  and  $l \in \mathbb{N}_L$ , we obtain:

$$\begin{aligned} z &= Hx, \\ \bar{z} &= \bar{H}\bar{x} \end{aligned} \quad (69)$$

where  $H \triangleq \text{diag}(H_i : i \in \mathbb{N}_N)$  and  $\bar{H} \triangleq \text{diag}(\bar{H}_l : l \in \mathbb{N}_L)$  represent the block diagonal matrices containing the output matrices of individual DGs and lines, respectively. This choice of output mapping provides a direct correspondence between system states and performance outputs.

To facilitate a comprehensive analysis of the entire MG, we define the consolidated performance output and disturbance vectors:

$$\begin{aligned} z_c &= [z^\top \quad \bar{z}^\top]^\top \\ w_c &= [w^\top \quad \bar{w}^\top]^\top. \end{aligned} \quad (70)$$

The consolidated disturbance vector  $w_c$  is mapped to the DG and line subsystems through the matrices  $E_c$  and  $\bar{E}_c$ , defined as:

$$\begin{aligned} E_c &= [E \quad \mathbf{0}] \\ \bar{E}_c &= [\mathbf{0} \quad \bar{E}] \end{aligned} \quad (71)$$

where  $E = \text{diag}(E_i : i \in \mathbb{N}_N)$  maps the DG disturbances  $w$  to the DG subsystems,  $\bar{E} = \text{diag}(\bar{E}_l : l \in \mathbb{N}_L)$  maps the line disturbances  $\bar{w}$  to the line subsystems, and the zero blocks indicate that line disturbances do not directly affect DG inputs and DG disturbances do not directly affect line inputs.

With these definitions, the interconnection relationship can be expressed as:

$$\begin{bmatrix} \tilde{u} \\ \tilde{u} \\ z_c \end{bmatrix} = M \begin{bmatrix} \tilde{x} \\ \tilde{x} \\ w_c \end{bmatrix} \quad (72)$$

where the interconnection matrix  $M$  takes the form:

$$M \triangleq \begin{bmatrix} M_{\tilde{u}x} & M_{\tilde{u}\bar{x}} & M_{\tilde{u}w_c} \\ M_{z_cx} & M_{z_c\bar{x}} & M_{z_cw_c} \end{bmatrix} \equiv \begin{bmatrix} K & \bar{C} & E_c \\ C & \mathbf{0} & \bar{E}_c \\ H_c & \bar{H}_c & \mathbf{0} \end{bmatrix}, \quad (73)$$

where  $H_c$  and  $\bar{H}_c$  are defined as:

$$\begin{aligned} H_c &= [H \quad \mathbf{0}]^\top, \\ \bar{H}_c &= [\mathbf{0} \quad \bar{H}]^\top, \end{aligned} \quad (74)$$

which map the DG and line states to the consolidated performance output  $z_c$ .

### A. Global Control and Topology Co-Design

The interconnection matrix  $M$  (30), particularly its block  $M_{\tilde{u}x} = K$ , can be synthesized by applying our subsystem EID properties to Prop. 3. By synthesizing  $K = [K_{ij}]_{i,j \in \mathbb{N}_N}$ , we can uniquely compute the distributed global controller gains  $\{k_{ij}^I : i, j \in \mathbb{N}_N\}$  (25) and the required communication topology  $\mathcal{G}^c$ . The following theorem formulates this distributed global controller and communication topology co-design problem.

**Theorem 4:** The closed-loop dynamics of the DC MG illustrated in Fig. 5 can be made finite-gain  $L_2$ -stable with an  $L_2$ -gain  $\gamma$  (where  $\tilde{\gamma} \triangleq \gamma^2 < \bar{\gamma}$  and  $\bar{\gamma}$  is prespecified) from unknown disturbances  $w_c(t)$  to performance output  $z_c(t)$ , by synthesizing the interconnection matrix block  $M_{\tilde{u}x} = K$  (30) via solving the LMI problem:

$$\begin{aligned} &\min_{\substack{Q, \{p_i : i \in \mathbb{N}_N\}, \\ \{\bar{p}_l : l \in \mathbb{N}_L\}, \tilde{\gamma}}} \sum_{i,j \in \mathbb{N}_N} c_{ij} \|Q_{ij}\|_1 + c_1 \tilde{\gamma} + \alpha \text{tr}(s_W), \\ \text{Sub. to: } &p_i > 0, \forall i \in \mathbb{N}_N, \bar{p}_l > 0, \forall l \in \mathbb{N}_L, \\ &0 < \tilde{\gamma} < \bar{\gamma}, \\ &W + s_W > 0, s_W \geq 0, \\ &\text{tr}(s_W) \leq \eta \text{ and (76),} \end{aligned} \quad (75)$$

as  $K = (\mathbf{X}_p^{11})^{-1}Q$ , where  $\mathbf{X}^{12} \triangleq \text{diag}([-\frac{1}{2\nu_i} \mathbf{I}]_{i \in \mathbb{N}_N})$ ,  $\mathbf{X}^{21} \triangleq (\mathbf{X}^{12})^\top$ ,  $\bar{\mathbf{X}}^{12} \triangleq \text{diag}([-\frac{1}{2\bar{\nu}_l} \mathbf{I}]_{l \in \mathbb{N}_L})$ ,  $\bar{\mathbf{X}}^{21} \triangleq (\bar{\mathbf{X}}^{12})^\top$ ,  $\mathbf{X}_p^{11} \triangleq \text{diag}([-p_i \nu_i \mathbf{I}]_{i \in \mathbb{N}_N})$ ,  $\mathbf{X}_p^{22} \triangleq \text{diag}([-p_i \rho_i \mathbf{I}]_{i \in \mathbb{N}_N})$ ,  $\bar{\mathbf{X}}_{\bar{p}}^{11} \triangleq \text{diag}([-\bar{p}_l \bar{\nu}_l \mathbf{I}]_{l \in \mathbb{N}_L})$ ,  $\bar{\mathbf{X}}_{\bar{p}}^{22} \triangleq \text{diag}([-\bar{p}_l \bar{\rho}_l \mathbf{I}]_{l \in \mathbb{N}_L})$ , and  $\tilde{\Gamma} \triangleq \tilde{\gamma} \mathbf{I}$ . The structure of  $Q \triangleq [Q_{ij}]_{i,j \in \mathbb{N}_N}$  mirrors that of  $K \triangleq [K_{ij}]_{i,j \in \mathbb{N}_N}$  (i.e., the first and third rows are zeros in each block  $Q_{ij}$ , see (25)). The coefficients  $c_1 > 0$  and  $c_{ij} > 0, \forall i, j \in \mathbb{N}_N$  are predefined cost coefficients corresponding to the  $L_2$ -gain from unknown disturbances and communication links respectively. Note that  $W$  represents the LMI matrix from (76),  $s_W$  is a symmetric slack matrix,  $\alpha > 0$  is the slack penalty weight, and  $\eta > 0$  is a bound on the total slack magnitude. Here  $\bar{\gamma}$  is the prespecified positive constant that represents the upper bounds on the  $L_2$ -gain for disturbance attenuation.

The symmetric slack matrix  $s_W$  provides numerical conditioning for the complex LMI constraints arising from the dissipativity conditions and interconnection requirements. The trace penalty term  $\alpha \text{tr}(s_W)$  in the objective function discourages excessive relaxation of the LMI constraints while maintaining feasibility. By bounding the trace of  $s_W$ , we ensure that any relaxation of the original stability conditions remains within acceptable limits determined by  $\eta$ . This formulation effectively balances the trade-off between numerical tractability and the fundamental stability and performance requirements of the DC MG.

Note that the proposed cost function in (75) jointly optimizes the communication topology (while inducing sparsity [23]) and robust stability (i.e.,  $L_2$ -gain  $\gamma$ ) of the DC MG.

### B. Necessary Conditions on Subsystem Passivity Indices

Based on the terms  $\mathbf{X}_p^{11}$ ,  $\mathbf{X}_p^{22}$ ,  $\bar{\mathbf{X}}_{\bar{p}}^{11}$ ,  $\bar{\mathbf{X}}_{\bar{p}}^{22}$ ,  $\mathbf{X}^{12}$ ,  $\mathbf{X}^{21}$ ,  $\bar{\mathbf{X}}^{12}$ , and  $\bar{\mathbf{X}}^{21}$  appearing in (76) included in the global co-design problem (75), it is clear that the feasibility and the effectiveness of this global co-design depend on the chosen passivity indices  $\{\nu_i, \rho_i : i \in \mathbb{N}_N\}$  (60) and  $\{\bar{\nu}_l, \bar{\rho}_l : l \in \mathbb{N}_L\}$  (61) assumed for DGs (23) and lines (21), respectively.

However, using Co. 1 for designing the local controllers

$$\begin{bmatrix} -p_i \nu_i & \mathbf{0} & \mathbf{0} & -p_i \nu_i \bar{C}_{il} \\ \mathbf{0} & -\bar{p}_l \bar{\nu}_l & -\bar{p}_l \bar{\nu}_l C_{il} & \mathbf{0} \\ \mathbf{0} & -C_{il} \bar{\nu}_l \bar{p}_l & p_i \rho_i & \frac{1}{2} p_i \nu_i \bar{C}_{il} + \frac{1}{2} C_{il}^\top \bar{\nu}_l \bar{p}_l \\ -\bar{C}_{il} \nu_i p_i & \mathbf{0} & \frac{1}{2} \bar{C}_{il}^\top \nu_i p_i + \frac{1}{2} \bar{p}_l \bar{\nu}_l C_{il} & \bar{p}_l \bar{\rho}_l \end{bmatrix} > 0 \quad (66)$$

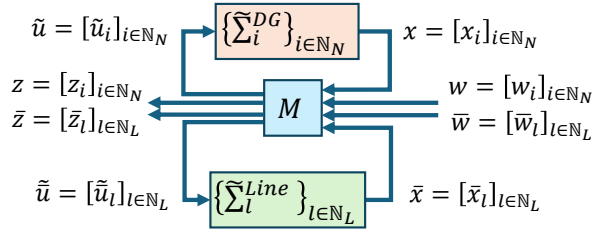


Fig. 5. DC MG error dynamics as a networked system with performance evaluation and disturbance rejection configuration.

in  $\{u_{iL} : i \in \mathbb{N}_N\}$  (13), we can obtain a custom set of passivity indices for the DGs (23). Similarly, using Lm. 2, we can obtain a custom set of passivity indices for the lines (21). Therefore, these local controller designs (Co. 1) and passivity analyses (Lm. 2) can impact the global co-design and potentially lead to infeasible and/or ineffective co-designs.

Therefore, when designing such local controllers and conducting passivity analysis, one must also consider the specific conditions necessary for the feasibility and effectiveness of the eventual global controller design. The following lemma identifies a few of such conditions based on (75) in Th. 4.

**Lemma 4:** For the LMI conditions in (75) in Th. 4 to hold, it is necessary that the DG and line passivity indices  $\{\nu_i, \rho_i : i \in \mathbb{N}_N\}$  (60) and  $\{\bar{\nu}_l, \bar{\rho}_l : l \in \mathbb{N}_L\}$  (61) are such that the LMI problem:

$$\begin{aligned} \text{Find:} & \quad \{(\nu_i, \rho_i, \tilde{\gamma}_i) : i \in \mathbb{N}_N\}, \{(\bar{\nu}_l, \bar{\rho}_l) : l \in \mathbb{N}_L\} \\ \text{Sub. to:} & \quad p_i > 0, \forall i \in \mathbb{N}_N, \bar{p}_l > 0, \forall l \in \mathbb{N}_L, \\ & \quad |w_i(t)| \leq \delta_i, \forall i \in \mathbb{N}_N, |\bar{w}_l(t)| \leq \delta_l, \forall l \in \mathbb{N}_L, \\ & \quad \text{and (77),} \end{aligned} \quad (78)$$

is feasible, where  $\delta_i$  and  $\delta_l$  are the bounds on the unknown disturbances for DGs and lines, respectively.

In conclusion, here we used the LMI constraints in (75) to derive a set of necessary LMI conditions as in (78).

### C. Local Controller Synthesis

To enforce the identified necessary LMI conditions in Lm. 4 (78) on DG and line passivity indices, a relaxed local controller synthesis problem is formulated. This ensures numerical feasibility while guaranteeing system stability. A slack variable  $s_{\bar{\rho}_l}$  is introduced to relax coupling constraints between DGs and lines, which mitigates numerical infeasibility while retaining strict passivity for individual subsystems.

**Theorem 5:** Under the predefined DG parameters (18), line parameters (21) and design parameters  $\{p_i : i \in \mathbb{N}_N\}$ ,  $\{\bar{p}_l : l \in \mathbb{N}_L\}$ , the necessary conditions in (75) hold if the local controller gains  $\{K_{i0}, i \in \mathbb{N}_N\}$  (13) and DG and line passivity indices  $\{\nu_i, \rho_i : i \in \mathbb{N}_N\}$  (60) and  $\{\bar{\nu}_l, \bar{\rho}_l : l \in \mathbb{N}_L\}$

(61) are determined by solving the LMI problem:

$$\min_{s_{\bar{\rho}}} \sum_{l=1}^L \alpha_{\bar{\rho}} s_{\bar{\rho}_l},$$

Find:  $\{(\tilde{K}_{i0}, P_i, \nu_i, \rho_i, \tilde{\gamma}_i) : i \in \mathbb{N}_N\}, \{(\bar{P}_l, \bar{\nu}_l, \bar{\rho}_l) : l \in \mathbb{N}_L\}$

Sub. to:  $|w_i(t)| \leq \delta_i, \forall i \in \mathbb{N}_N, |\bar{w}_l(t)| \leq \delta_l, \forall l \in \mathbb{N}_L,$

$$P_i > 0, \begin{bmatrix} \bar{\rho}_i \mathbf{I} & P_i & \mathbf{0} \\ P_i & -\mathcal{H}(A_i P_i + B_i \tilde{K}_{i0}) & -\mathbf{I} + \frac{1}{2} P_i \\ \mathbf{0} & -\mathbf{I} + \frac{1}{2} P_i & -\nu_i \mathbf{I} \end{bmatrix} > 0, \forall i \in \mathbb{N}_N,$$

$$\bar{P}_l > 0, \begin{bmatrix} \frac{2\bar{P}_l \bar{R}_l}{L_l} - \bar{\rho}_l & -\frac{\bar{P}_l}{L_l} + \frac{1}{2} \\ * & -\bar{\nu}_l \end{bmatrix} \geq 0, \forall l \in \mathbb{N}_L,$$

and (77),

where  $K_{i0} \triangleq \tilde{K}_{i0} P_i^{-1}$ ,  $s_{\bar{\rho}_l} \geq 0$  is the slack variable for coupling constraints,  $\alpha_{\bar{\rho}}$  is its associated penalty weight, and the  $\delta_i$  and  $\delta_l$  are the bounds on DG and line disturbances, respectively.

The slack variable  $s_{\bar{\rho}_l}$  serves to relax only the coupling constraints between DGs and lines while maintaining the strict passivity properties of individual subsystems. By introducing relaxation only in the interconnection terms, we preserve the core passivity properties of both DGs and lines while providing numerical feasibility for the optimization problem. The weighted objective function includes the slack variable penalty. The penalty weight on the slack variable ensures that the relaxation is used minimally, only when necessary to achieve feasibility.

### D. Overview

In the proposed co-design process, we first select the design parameters  $p_i, \forall i \in \mathbb{N}_N$  and  $\bar{p}_l, \forall l \in \mathbb{N}_L$  (for more details, see [22]). Next, we synthesize the local controllers using Th. 5, to obtain DG and line passivity indices  $\{\rho_i, \nu_i : \forall i \in \mathbb{N}_N\}$  (60) and  $\{\bar{\rho}_l, \bar{\nu}_l : \forall l \in \mathbb{N}_L\}$  (61), respectively. Finally, we synthesize the distributed global controller and the communication topology of the DC MG using Th. 4.

## VII. SIMULATION RESULTS

This section presents the simulation results for evaluating the proposed dissipativity-based control and topology co-design method. Currently, we are in the process of finalizing the simulations and validating the results. The experiments involve an islanded DC MG with different configurations, subjected to various load variations to assess the performance of the designed controllers. We are conducting extensive tests to ensure the accuracy and robustness of the proposed approach. The detailed results and performance analysis will be provided in a future version of this manuscript.

## VIII. CONCLUSION

This paper proposes a dissipativity-based distributed droop-free control and communication topology co-design approach for DC MGs. By leveraging dissipativity theory, we develop a unified framework that simultaneously addresses the distributed global controller design and the communication topology design problems. To support the feasibility of this global co-design process, we use specifically designed

local controllers at the subsystems. We formulate all design problems as LMI-based convex optimization problems to enable efficient and scalable evaluations. Using a distributed droop-free controller over an optimized communication topology, the proposed approach ensures robust voltage regulation and current sharing for various disturbances. Future work will focus on developing a decentralized and compositional co-design framework enabling seamless plug-and-play behaviors.

## REFERENCES

- [1] Y. Wang, T. L. Nguyen, Y. Xu, Z. Li, Q.-T. Tran, and R. Caire, "Cyber-physical Design and Implementation of Distributed Event-Triggered Secondary Control in Islanded Microgrids," *IEEE Transactions on Industry Applications*, vol. 55, no. 6, pp. 5631–5642, 2019.
- [2] M. Mehdi, C.-H. Kim, and M. Saad, "Robust Centralized Control for DC Islanded Microgrid Considering Communication Network Delay," *IEEE Access*, vol. 8, pp. 77 765–77 778, 2020.
- [3] A. Khorsandi, M. Ashourloo, and H. Mokhtari, "A Decentralized Control Method for a Low-Voltage DC Microgrid," *IEEE Transactions on Energy Conversion*, vol. 29, no. 4, pp. 793–801, 2014.
- [4] V. Nasirian, S. Moayedi, A. Davoudi, and F. L. Lewis, "Distributed Cooperative Control of DC Microgrids," *IEEE Transactions on Power Electronics*, vol. 30, no. 4, pp. 2288–2303, 2014.
- [5] J. M. Guerrero, J. C. Vasquez, J. Matas, L. G. De Vicuña, and M. Castilla, "Hierarchical Control of Droop-Controlled AC and DC Microgrids—A General Approach Toward Standardization," *IEEE Transactions on industrial electronics*, vol. 58, no. 1, pp. 158–172, 2010.
- [6] T. Morstyn, B. Hredzak, G. D. Demetriades, and V. G. Agelidis, "Unified Distributed Control for DC Microgrid Operating Modes," *IEEE Transactions on Power Systems*, vol. 31, no. 1, pp. 802–812, 2015.
- [7] N. M. Dehkordi, N. Sadati, and M. Hamzeh, "Distributed Robust Finite-Time Secondary Voltage and Frequency Control of Islanded Microgrids," *IEEE Transactions on Power systems*, vol. 32, no. 5, pp. 3648–3659, 2016.
- [8] Q. Zhang, Y. Zeng, Y. Hu, Y. Liu, X. Zhuang, and H. Guo, "Droop-Free Distributed Cooperative Control Framework for Multisource Parallel in Seaport DC Microgrid," *IEEE Transactions on Smart Grid*, vol. 13, no. 6, pp. 4231–4244, 2022.
- [9] Q. Zhou, M. Shahidehpour, A. Paaso, S. Bahramirad, A. Alabdulwahab, and A. Abusorrah, "Distributed Control and Communication Strategies in Networked Microgrids," *IEEE Communications Surveys & Tutorials*, vol. 22, no. 4, pp. 2586–2633, 2020.
- [10] V. Nasirian, A. Davoudi, and F. L. Lewis, "Distributed Adaptive Droop Control for DC Microgrids," in *2014 IEEE Applied Power Electronics Conference and Exposition-APEC 2014*. IEEE, 2014, pp. 1147–1152.
- [11] M. J. Najafirad, N. M. Dehkordi, M. Hamzeh, and H. Nazaripouya, "Distributed Event-Triggered Control of DC Microgrids With Input Saturation and Time Delay Constraints," *IEEE Systems Journal*, 2023.
- [12] J. Lofberg, "YALMIP : A Toolbox for Modeling and Optimization in MATLAB," in *Proc. of IEEE Intl. Conf. on Robotics and Automation*, 2004, pp. 284–289.
- [13] S. Welikala, H. Lin, and P. J. Antsaklis, "Non-Linear Networked Systems Analysis and Synthesis using Dissipativity Theory," in *2023 American Control Conference (ACC)*. IEEE, 2023, pp. 2951–2956.
- [14] S. Welikala, H. Lin, and P. Antsaklis, "A Generalized Distributed Analysis and Control Synthesis Approach for Networked Systems with Arbitrary Interconnections," in *2022 30th Mediterranean Conference on Control and Automation (MED)*. IEEE, 2022, pp. 803–808.
- [15] M. Arcak, "Compositional Design and Verification of Large-Scale Systems Using Dissipativity Theory: Determining Stability and Performance From Subsystem Properties and Interconnection Structures," *IEEE Control Systems Magazine*, vol. 42, no. 2, pp. 51–62, 2022.
- [16] S. Welikala, H. Lin, and P. J. Antsaklis, "On-line Estimation of Stability and Passivity Metrics," in *Proc. of 61st IEEE Conf. on Decision and Control*, 2022, pp. 267–272.
- [17] S. Welikala, Z. Song, P. J. Antsaklis, and H. Lin, "Dissipativity-Based Decentralized Co-Design of Distributed Controllers and Communication Topologies for Vehicular Platoons," *arXiv preprint arXiv:2312.06472*, 2023.
- [18] P. Nahata, R. Soloperto, M. Tucci, A. Martinelli, and G. Ferrari-Trecate, "A Passivity-Based Approach to Voltage Stabilization in DC Microgrids With ZIP Loads," *Automatica*, vol. 113, p. 108770, 2020.
- [19] F. Dorfler and F. Bullo, "Kron Reduction of Graphs With Applications to Electrical Networks," *IEEE Transactions on Circuits and Systems I: Regular Papers*, vol. 60, no. 1, pp. 150–163, 2012.
- [20] P. Kundur, "Power System Stability," *Power system stability and control*, vol. 10, pp. 7–1, 2007.
- [21] M. Tucci, S. Rivero, and G. Ferrari-Trecate, "Line-Independent Plug-and-Play Controllers for Voltage Stabilization in DC Microgrids," *IEEE Transactions on Control Systems Technology*, vol. 26, no. 3, pp. 1115–1123, 2017.
- [22] M. J. Najafirad and S. Welikala, "Distributed Dissipativity-Based Controller and Topology Co-Design for DC Microgrids," *arXiv e-prints*, p. 2404.18210, 2024. [Online]. Available: <http://arxiv.org/abs/2404.18210>
- [23] R. Jenatton, J.-Y. Audibert, and F. Bach, "Structured Variable Selection with Sparsity-Inducing Norms," *The Journal of Machine Learning Research*, vol. 12, pp. 2777–2824, 2011.

$$W = \begin{bmatrix} \mathbf{X}_p^{11} & \mathbf{0} & \mathbf{0} & \mathbf{Q} & \mathbf{X}_p^{11} \bar{\mathbf{C}} & \mathbf{X}_p^{11} \mathbf{E}_c \\ \mathbf{0} & \bar{\mathbf{X}}_p^{11} & \mathbf{0} & \bar{\mathbf{X}}_p^{11} \mathbf{C} & \mathbf{0} & \bar{\mathbf{X}}_p^{11} \bar{\mathbf{E}}_c \\ \mathbf{0} & \mathbf{0} & \mathbf{I} & \mathbf{H}_c & \mathbf{0} & \mathbf{0} \\ \mathbf{Q}^\top & \mathbf{C}^\top \bar{\mathbf{X}}_p^{11} & \mathbf{H}_c^\top & -\mathbf{Q}^\top \mathbf{X}^{12} - \mathbf{X}^{21} \mathbf{Q} - \mathbf{X}^{22} & -\mathbf{X}^{21} \mathbf{X}_p^{11} \bar{\mathbf{C}} - \mathbf{C}^\top \bar{\mathbf{X}}_p^{11} \bar{\mathbf{X}}^{12} & -\mathbf{X}^{21} \mathbf{X}_p^{11} \mathbf{E}_c \\ \bar{\mathbf{C}}^\top \mathbf{X}_p^{11} & \mathbf{0} & \bar{\mathbf{H}}_c^\top & -\bar{\mathbf{C}}^\top \mathbf{X}_p^{11} \mathbf{X}^{12} - \bar{\mathbf{X}}^{21} \bar{\mathbf{X}}_p^{11} \mathbf{C} & -\bar{\mathbf{X}}^{22} & -\bar{\mathbf{X}}^{21} \bar{\mathbf{X}}_p^{11} \bar{\mathbf{E}}_c \\ \mathbf{E}_c^\top \mathbf{X}_p^{11} & \bar{\mathbf{E}}_c^\top \bar{\mathbf{X}}_p^{11} & \mathbf{0} & -\mathbf{E}_c^\top \mathbf{X}_p^{11} \mathbf{X}^{12} & -\bar{\mathbf{E}}_c^\top \bar{\mathbf{X}}_p^{11} \bar{\mathbf{X}}^{12} & \bar{\Gamma} \end{bmatrix} > 0 \quad (76)$$

$$\begin{bmatrix} -p_i \nu_i & 0 & 0 & 0 & -p_i \nu_i \bar{\mathbf{C}}_{il} & -p_i \nu_i \\ 0 & -\bar{p}_i \bar{\nu}_i & 0 & -\bar{p}_i \bar{\nu}_i C_{il} & 0 & 0 \\ 0 & 0 & 1 & H_{ci} & \bar{H}_{cl} & 0 \\ 0 & -C_{il} \bar{\nu}_i \bar{p}_i & H_{ci} & p_i \rho_i & \frac{1}{2} p_i \nu_i \bar{\mathbf{C}}_{il} + \frac{1}{2} C_{il} \bar{\nu}_i \bar{p}_i & \frac{1}{2} p_i \nu_i \\ -\bar{\mathbf{C}}_{il} \nu_i p_i & 0 & \bar{H}_{cl} & \frac{1}{2} \bar{\mathbf{C}}_{il} \nu_i p_i + \frac{1}{2} \bar{p}_i \bar{\nu}_i C_{il} & p_i \rho_i & 0 \\ -\nu_i p_i & 0 & 0 & \frac{1}{2} \nu_i p_i & 0 & \tilde{\gamma}_i \end{bmatrix} > 0 \quad (77)$$